Multi-Objective Design of Post-Tensioned Concrete Road Bridges Using Artificial Neural Networks

Tatiana García-Segura[1], Víctor Yepes[2], Dan M. Frangopol[3]

Abstract

In order to minimize the total expected cost, bridges have to be designed for safety and durability. This paper considers the cost, the safety, and the corrosion initiation time to design post-tensioned concrete box-girder road bridges. The deck is modeled by finite elements based on problem variables such as the cross-section geometry, the concrete grade, and the reinforcing and post-tensioning steel. An integrated multi-objective harmony search with artificial neural networks (ANNs) is proposed to reduce the high computing time required for the finite-element analysis and the increment in conflicting objectives. ANNs are trained through the results of previous bridge performance evaluations. Then, ANNs are used to evaluate the constraints and provide a direction towards the Pareto front. Finally, exact methods actualize and improve the Pareto set. The results show that the harmony search parameters should be progressively changed in a diversification-intensification strategy. This methodology provides trade-off solutions that are the cheapest ones for the safety and durability levels considered. Therefore, it is possible to choose an alternative that can be easily adjusted to each need.

Keywords: Multi-objective harmony search; artificial neural networks; post-tensioned concrete bridges; durability; safety

---

[1] Graduate Research Assistant, Institute of Concrete Science and Technology (ICITECH), *Universitat Politècnica de València*, 46022 Valencia, Spain. **Corresponding author**. Phone +34963879563; Fax: +34963877569; E-mail: tagarse@cam.upv.es

[2] Associate Professor, Institute of Concrete Science and Technology (ICITECH), *Universitat Politècnica de València*, 46022 Valencia, Spain. E-mail: vyepesp@cst.upv.es

[3] Professor and the Fazlur R. Khan Endowed Chair of Structural Engineering and Architecture, Department of Civil and Environmental Engineering, Engineering Research Center for Advanced Technology for Large Structural Systems (ATLSS Center), *Lehigh University*, 117 ATLSS Dr., Bethlehem, PA 18015-4729, USA. E-mail: dan.frangopol@lehigh.edu

1. Introduction

Optimization methods provide an effective alternative to structural designs based on experience. Metaheuristic or stochastic algorithms use a combination of rules and randomness to effectively search large discrete variable spaces to find an optimal solution. Reviews on non-heuristic and heuristic algorithms applied to structural optimization can be found, respectively, in Sarma and Adeli (1998) and Hare et al. (2013). Regarding multi-objective optimization, Zavala et al. (2013) presented a survey of multi-objective metaheuristics applied to structural optimization. There are numerous examples of heuristic algorithms that have been applied to civil and structural engineering, such as Genetic Algorithm (GA) (Cai and Aref 2015), Memetic Algorithm (MA) (Martí et al. 2015), Simulated Annealing (SA) (Quaglia et al. 2014; Martí et al. 2016), Particle Swarm Optimization (PSO) (Sreehari and Maiti 2016), Glowworm Swarm Optimization (GSO) (García-Segura et al. 2014b; Yepes et al. 2015b), Harmony Search (HS) (Martini 2011; García-Segura et al. 2015), among others. Alberdi and Khandelwal (2015) performed a thorough discussion in the light of the results of a comparison of ACO, GA, HS, PSO, SA, and TS and three improved variants. The best results were obtained in the design-driven HS. The algorithm was shown to be robust in optimization problems with large and poorly organized variable spaces. In addition, these authors highlighted the importance of diversification and intensification.

Traditionally, engineers have aimed at reducing the weight and cost of structures. However, concerns regarding building a more sustainable future have led to the incorporation of criteria like environmental impact, durability, and safety level, among others. García-Segura et al. (2014a) studied the life-cycle greenhouse gas emissions of concrete columns, taking into account carbonation and durability. Paya et al. (2008) considered that reinforced concrete (RC) building frames should be studied according to the economic cost, the constructability, the environmental impact, and the overall safety. Similar criteria were used to design RC bridge piers (Martinez-Martin et al. 2012), and pavements (Torres-Machi et al. 2015). Yepes et al. (2015a) incorporated the prediction of service life as a criterion in the design of a high-strength RC I-beam. García-Segura and Yepes (2016) found designs of the post-tensioned concrete box-girder road bridge that represent optimal trade-offs among the cost, CO_2 emissions, and overall safety factor.

Multi-objective optimization is used as a tool to find multiple trade-off solutions. However, a large computational time is required to evaluate solutions to certain problems. This is due to the existence of many decision variables or the evaluation procedure, like the use of the finite element method or a network flow computation (Deb and Nain 2007). Meta-models for objective functions and constraints have been developed for this purpose (Deb 2011). Giannakoglou (2002) claimed that optimization methods based on stochastic require huge time and demonstrated the usefulness of surrogate or approximation models. Emmerich and Naujoks (2004) presented various metamodel-assisted multi-objective evolutionary algorithms based on Gaussian field (Kriging) models. Deb and Nain (2007) studied the possibility of using approximate models like artificial neural networks (ANNs) in multi-objective optimization. The results showed a saving in exact function evaluations of about 25 to 62%.

ANN is a machine learning method based on artificial neurons. The ANN learns from the training examples and provides a response or output by approximating non-linear functions of their inputs. ANN has been performed to analyze several topics related to civil engineering. Authors aim to predict structural behavior (Sanad and Saka 2001; Marti-Vargas et al. 2013), to analyze the effects of the input parameters on the output (Zavrtanik et al. 2016; Shi 2016), and to study the sensitivity of parameters (Cao et al. 2015). Chatterjee et al. (2016) employed ANN for structural failure prediction. In this line, Protopapadakis et al. (2016) presented a neural detector aimed at identifying the structural defects in concrete piles.

As mentioned previously, structures are designed according to the appropriate criteria for each particular case. In this case, multi-objective optimization is applied by simultaneously minimizing the cost and maximizing the overall safety factor and the corrosion initiation time. Cost optimization is essential to achieve a good design with the minimum economic resources. Safety can be analyzed when the structure is expected to be under increased loads or the deterioration process may cause a reduction in structural safety. Corrosion initiation is included as objective function for further deepening in the durability requirements. Despite durability is a more common criterion when the management phase is studied, aspects related to future performance are gaining increased attention in the design and assessment of structures (Dong et al. 2013). In this regard, this paper considers the durability objective in the design phase with the aim of designing for longevity and reduced long-term impacts. Note that designers sometimes need to analyze the same structure with different criteria and the computing time increases with the number of objectives studied.

In this paper, ANN is integrated in a multi-objective HS to reduce the high computational cost needed to evaluate the constraints of a real bridge optimization problem. This methodology is applied to a post-tensioned concrete (PSC) box-girder road bridge located in a coastal region. The bridge design is defined by 34 variables which determine the cross-section geometry, the concrete grade, the reinforcement and post-tensioning steel. The deck is evaluated by using finite elements. Shell elements are used to generate the finite element model. The trained ANN is used to predict the structural response in terms of the limit states based on the design variables, without the need to analyze the bridge response. After this process, the Pareto set is actualized and improved through exact analysis. Finally, the multi-objective optimization provides bridge managers with a complete set of alternative trade-off solutions with respect to cost, overall safety factor, and corrosion initiation time.

2. Bridge design optimization

Bridge optimization is formulated to minimize the cost and maximize the overall safety factor and the corrosion initiation time by providing the optimum PSC box-girder cross-section bridge design according to the variables and parameters. In this paper, bridge design optimization is studied. The bridge has three continuous spans with a main span (L_1) of 44 m and external span (L_2) of 35.2 m. The deck has a width of 11.8 m. The bridge is located in a coastal region. Figure 1 shows the bridge elevation. A total of 34 variables define the cross-section geometry, the concrete, and the reinforcing and post-tensioning steel of the bridge. The depth (h), the width of the bottom slab (b), the width of the web inclination (d), the thickness of the top slab (e_s), the thickness of the external flange section (e_v), the thickness of the internal flange section (e_{va}), the thickness of the bottom slab (e_i), the thickness of the webs (e_a), and the concrete cover (c_c) form the geometric variables. Note that the web inclination is determined according to the web slope, which takes values between 2 and 4, and the minimum concrete cover is fixed at 30 mm. Other dimensions, like t_1, t_2, t_3, and t_4 (see Fig. 2), depend on the values of the variables (Eqs. (1–4)).

$$t_1 = e_{va} - e_s \qquad (1)$$

$$t_2 = \frac{b+2*d}{5} \qquad (2)$$

$$t_3 = e_i \qquad (3)$$

$$t_4 = \frac{b}{10} \qquad (4)$$

The concrete strength (f_{ck}) takes values from 35 to 100 MPa. Post-tensioning is applied by the use of post-tensioning tendons, which form a parabolic layout symmetrically distributed through the webs. Three variables define the post-tensioning system: the eccentricity in the external spans (e_p) as a percentage of half of the depth, the distance from the piers to the point of inflection (L_{pi}) as a percentage of the span length, and the number of strands (N_S). The eccentricity in the supports and the midspan of the central span are the maximum allowed. Likewise, the prestressing force in each strand is specified as 195.52 KN. Regarding the duct placement, while the ducts are allocated in a line over the piers, they are placed in rows of two in the lower points of the layout.

The last variables deal with the reinforcement. The longitudinal reinforcing steel is defined by the diameter (LR_1, LR_2, LR_3, LR_4, LR_5, LR_6, LR_7, LR_8, LR_9, LR_{10}) and the number of bars (N_{LR}) per meter which is the same for all the bars. The deck is divided into two zones: the piers (L/5 on both sides of the piers) and the rest of the span. An extra reinforcement is placed in the top slab (LR_7, LR_8) and in the bottom slab (LR_9, LR_{10}) along the two zones. Similarly, the diameter (TR_1, TR_2, TR_3, TR_4, $TR_{4'}$, TR_5, TR_6, TR_7, TR_8) and spacing (S_{TR}) determine the transverse reinforcement. $TR_{4'}$ is an extra reinforcement placed at the same position as TR_4 to covers the support zone (L/5 on both sides of all supports). TR_8 is an extra reinforcement over the flanges. TR9 is not a variable, since it is fixed as 12 mm.

Once the values of the variables have been defined, the bridge design is completed and the verification module can check the feasibility of the structural constraints. Spanish codes for actions (Fomento 2011) and concrete evaluation (Fomento 2008), which are based on the Eurocode (European Committee for Standardisation 2003; European Committee for Standardisation 2005), are used. Actions considered are the traffic loads defined in the code, the self-weight, the parapet (5 KN/m) and asphalt (24 KN/m^3) loads, the thermal gradient of the code, differential settling in each support (5 mm), and the post-tensioned steel effect. The constraints check the ultimate and serviceability limit states of flexure, shear, shear between web and flanges, torsion, stresses, and deflection. As the bridge is located in a coastal region, the decompression limit state checks that the concrete located 100 mm above and under the strands is not in tension (European Committee for Standardisation 2005). Two deflection verifications check whether the instantaneous and time-dependent deflection with respect to the pre-camber is smaller than 1/1400 of the main span length for the characteristic combination (Fomento 2008) and whether the frequent value for the live loads is smaller than 1/1000 of the main span length (Fomento 2011). Besides, geometrical and constructability requirements are also considered.

Bridge dimensions and loads are modeled in CSiBridge©(Computers and Structures Inc). A linear analysis by finite elements is carried out. The PSC box-girder is represented by shell elements that contain an embedded reinforcement grid. The prestressed tendons are also incorporated into the model. The study considers the instantaneous and deferred losses, which are used to evaluate the prestressing force at the tensioning stage and at final life. Diaphragms are assigned over each support. The finite element mesh considers a maximum segment length for discretization information of 3 m and a maximum submesh size of 1.5 m. Besides, a section cut is always applied over supports and every change in thickness of the transverse section is a condition for a finite element division.

CSiBridge© is linked with Matlab© to create the model with the bridge information and extract the results of the structural analysis. CSiBridge© has an Open Application Programming Interface (OAPI) to allow other software to be integrated with it. CSiBridge© is used for the finite-element analysis. Matlab© is used to control the finite-element analysis, check the limit states and evaluate the objective functions. The program is comprised of eight modules. Module 1 updates the design variables based on the algorithm strategy. Module 2 completes the design with the variable and parameter information. In addition, this module evaluates the section properties required for the limit state checking. Module 3 writes a $br document with the structure information. Module 4 imports the $br document and runs the model. Module 5 extracts the results by OAPI functions. Module 6 processes the previous analysis results, evaluates the bridge resistance, and checks the limit states. Module 7 evaluates the objective functions. Finally, Module 8 obtains the Pareto optimum solutions. This is repeated for each iteration of the optimization process.

2. 1. Objective functions

2.1.1. Cost

The cost (C) is evaluated as:

$$C = C_c \cdot V_c + C_{rs} \cdot W_{rs} + C_{ps} \cdot W_{ps} + C_f \cdot A_f \qquad (5)$$

where C_c is the unit cost of concrete, V_c is the volume of concrete, C_{rs} is the unit cost of reinforcing steel, W_{rs} is the weight of reinforcement steel, C_{ps} is the unit cost of prestressing steel, W_{ps} is the weight of prestressing steel, C_f is the unit cost of formwork, and A_f is the area of the formwork. The unit cost of the materials includes raw material extraction, manufacture, and transportation. More details are included in Garcia-Segura et al. (2015). Table 1 summarizes the unit costs for each material.

2.1.2. Safety

The overall safety factor (S) calculated according to the Spanish code (Fomento 2008; Fomento 2011) and Eurocode (European Committee for Standardisation 2003; European Committee for Standardisation 2005), is as follows:

$$S(\vec{x}) = Minimum\ \gamma_j(\vec{x}),\ \ \mathrm{j} = 1, \dots, \mathrm{n} \qquad (6)$$

where γ_j is the safety coefficient of ultimate limit states, n is the number of ultimate limit states considered and the vector x contains the design variables. This coefficient (γ_j) is obtained as the ratio between the factored ultimate resistance of the structural response and the factored ultimate load effect of actions considering the partial safety factors in the codes (Fomento 2008; Fomento 2011). A safety coefficient of one represents strict compliance with the code. Torsion, flexure, transverse flexure, and shear limit states are all taken into account. Therefore, the number of ultimate limit states (n) is four.

2.1.3. Corrosion initiation time

The corrosion initiation time (t_{corr}) is the time required for the chloride concentration on the surface of the reinforcing steel, which coincides with the concrete cover, to reach a critical threshold value (C_r). The chloride content at a distance x from the outer surface of concrete at time t is calculated based on Fick´s second law as:

$$C(x,t) = Co\left[1 - \mathrm{erf}\left(\frac{x}{2\sqrt{tD}}\right)\right] \quad (7)$$

where C_o is the chloride concentration on the surface, D is the apparent diffusion coefficient, and erf is the error function. The uncertainties related to the surface content, apparent diffusion coefficient, concrete cover, and critical threshold value are considered through random variables shown in Table 2. The parameters of random variables are those used by Vu and Stewart (2000), except for the coefficient of variation (COV) of the surface chloride content, which is considered 0.3 due to the reduction of the variability of the surface chloride content in a particular bridge compared to a group of bridges. The surface chloride content depends on the distance to the coast. The mean value is 2.95 kg/m^3 for a distance of up to 1000 m from the coast (McGee 1999).

The diffusion coefficient (D) depends on the concrete permeability.

$$D = D_{H_2O} 0.15 \cdot \frac{1+\rho_c \frac{w}{c}}{1+\rho_c \frac{w}{c}+\frac{\rho_c a}{\rho_a c}} \left(\frac{\rho_c \frac{w}{c} - 0.85}{1+\rho_c \frac{w}{c}} \right)^3 \qquad (8)$$

Vu and Stewart (2000) suggested the model developed by Papadakis et al. (1996) (see Eq. (8)), which depends on the chloride diffusion coefficient in an infinite solution (D_{H20} = 1.6*10^{-5} cm^2/s for NaCl), the mass density of cement (ρ_c, assumed to be 3.16 g/cm^3), the mass density of the aggregates (ρ_a, assumed to be 2.6 g/cm^3), the aggregate-to-cement ratio (*a/c*), and the water-cement ratio (*w/c*). Table 3 shows the values according to the concrete grades. The corrosion initiation time distribution is obtained by Monte Carlo simulation. This method randomly selects values of the variables associated with corrosion and calculates the output using Eq. (7) and (8). This process is repeated during 10000 iterations. The mean value of the lognormal distribution is given as the representative value.

2.2. Optimization method

The proposed method encompasses two models. The first is an approximate model to guide the optimization process and provide a near-optimum Pareto front. An ANN is integrated in a multi-objective HS for this task. The ANN is trained using data collected from previous studies. The trained ANN is used to predict the limit state coefficients from the design variables, as the large computational time of a multi-objective bridge optimization is due to the structural analysis. The limit state coefficients evaluate the ratio between the factored resistance of the structural response or the permitted limit value for the limit state and the factored load effect of actions for this limit state. Secondly, a multi-objective optimization with a complete bridge analysis and verification actualizes and improves the Pareto set through exact evaluation. This combination of models aims to reduce the computing time while achieving a good performance. Trade-offs between cost, safety, and corrosion initiation are obtained through this method.

The ANN consists of many processing elements or neurons that use a backpropagation algorithm. The model learns from the input elements by adjusting the weights through an iterative process in which the model outputs are compared with measured outputs and the errors are back-propagated. The multilayer feedforward network is formed by one hidden layer of sigmoid neurons followed by an output layer of linear neurons. Neurons of the hidden layer are connected to all neurons in the input and output layers (see Fig 3). The number of neurons in the input and output layers corresponds with the number of input and output parameters. Inputs (x_i) are multiplied by weights ($w_{i,j}$) and combined linearly with an independent term or bias (b). Each hidden neuron follows this equation ($\sum x_i \cdot w_{i,j} + b$). Then, each neuron of the hidden layer produces an output by applying a tan-sigmoid function to the linear combination. The output layer follows the same procedure, but applying a linear function. The mean square error (MSE) and the coefficient of determination (R^2) are used to check the accuracy of the network.

The HS algorithm was proposed by Geem et al. (2001) based on the process of searching for the perfect musical harmony; equivalently, the heuristic algorithm searches for the best solution. This algorithm uses the following parameters: the harmony memory size (HMS) or number of solution vectors, the harmony memory considering rate (HMCR), and the pitch adjusting rate (PAR). Later, a multi-objective version of the HS algorithm was proposed by Xu et al.(2010). Ricart et al. (2011) presented two proposals for the multi-objective HS. This paper uses the second proposal, as Ricart et al. (2011) found that the algorithm is competitive even when compared to NSGA-II (Non-dominated Sorting Genetic Algorithm II). In addition, the crowding distance criterion is considered to select solutions with the same ranking. This criterion benefits the diversification, since the solutions with greater crowding distance are those further from other solutions. The crowding distance measures the perimeter of the cuboid formed by the nearest neighbors in the objective space as the vertices. This algorithm was explained in detail in García-Segura and Yepes (2016).

Two important components of most stochastic search algorithms are diversification and intensification (Alberdi and Khandelwal 2015). Diversification makes it possible to explore the entire design space and avoids trapping in local optima. However, intensification is also needed to improve the convergence. This paper checks several intensification-diversification strategies by changing the algorithm parameters. HS generates new designs from parts of other good designs registered in the harmony memory (HM). Fixing the memory consideration to a unique random HM solution, instead of combining solutions, is studied. Besides, HMCR is modified to vary the choice of the values of the variables randomly. Increasing the value of HMCR reduces the random selection. When HMCR is equal to one, the algorithm just perturbs parts of existing designs according to PAR. The cases studied are explained in Section 2.2.2.

Moreover, the use of penalty functions is studied. When ANN is integrated in a multi-objective HS, approximate solutions are obtained. In this context, unfeasible solutions can be feasible after the exact evaluation. Thus, penalties are studied for the unfeasible solutions to worsen their aptitude. This approach transforms the constrains related to the limit states in penalized objective values, which are small for light lacks of compliance and strong for larger ones. A review of penalty functions can be found in the study of Coello (2002). The penalty function used is $F_p = (K_p/f)\cdot F$, where F_p is the penalized cost; F is the non-penalized cost; f is equal to the minimum limit state coefficient, and K_p is an extra coefficient. Other penalty functions were tried without improving the convergence to the minimum. As f is a coefficient of unfeasibility with a value of less than one, the objective functions are penalized according to degree of compliance. In addition, an extra coefficient K_p worsen the value of unfeasible solutions. This coefficient reduces the divergence caused by the high sensitivity of the unfeasible prestressed concrete structures. Two options for the K_p coefficient are studied (see Table 4).

This paper uses the hypervolume measure to compare different Pareto fronts and establish a termination criterion. The hypervolume measure is a frequently applied quality measure for comparing the results of multi-objective optimization algorithms. Coello et al. (2006) reported a variety of indicators to measure the quality of Pareto front approximations. Among them, the hypervolume measure or S-metric is of outstanding importance (Beume et al. 2007). This quality indicator rewards the convergence towards the Pareto front as well as the representative distribution of points along the front. The hypervolume measure was originally proposed by Zitzler and Thiele (1998), who called it the size of dominated space. Then, it was described as the Lebesgue measure. To evaluate the hypervolume, the values are firstly normalized. As the problem is established as a minimization of the cost and the negative value of corrosion initiation time and the overall safety factor, the values are divided by (20x10^6, 500, 2) and the utopia and antiutopia points are (0, –1, –1) and (1, 0, 0).

The proposed method is divided into four steps, as Fig. 4 shows.

2.2.1 Step 1. ANN training

The neural network is trained using 4500 data, which comprise the 34 input variables and one output variable. The output variable refers to the limit state coefficients. These data are obtained through the exact method. CSiBridge© is used for the finite-element analysis and Matlab© verifies the limit states based on the load effects obtained from CSiBridge© and the bridge resistance evaluation. As there are 17 limit states or output variables, the process is repeated 17 times and 17 ANNs are obtained. The data are divided into training (70%), validation (15%), and test (15%) sets. The ANN uses a Levenberg-Marquardt backpropagation algorithm with 10 neurons. The number of neurons was adjusted to provide the best performance. This process is finalized when the number of iterations reaches 1000, or the performance function drops below 10^{-8}, or the magnitude of the gradient is less than 10^{-10}, or the maximum number of validation failures exceeds 50.

2.2.2 Step 2. Approximate Pareto set.

A multi-objective HS is combined with ANN to minimize the cost and maximize the corrosion initiation time and the overall safety factor while complying with the constraints. ANN is used to obtain the coefficient of the limit states from the design variables. Each simulation is carried out nine times and the average value is obtained. These values are used to evaluate the constraints and the overall safety factor. The constraints check whether the coefficients of the limit states are greater than one. The overall safety factor is obtained according to Eq. (6). This process is performed for 20000 iterations, since the hypervolume of the Pareto front tends to stabilize around this value (see Fig. 5). Besides, to improve the efficiency of the algorithm, different cases regarding diversification-intensification strategies and penalty functions are considered (see Table 4). Note that these values have been selected based on the results of García-Segura et al. (2015). These authors used a Design of Experiments methodology to propose HMS=200, HMCR=0.7 and PAR=0.4 as the algorithm parameters.

2.2.3 Step 3. Updated Pareto set

Step 3 involves the update of the Pareto set. The solutions registered in the HM are updated, with the Pareto set of solutions being among them. HM is formed by approximate solutions, which are actualized to depart from exact solutions. To this end, CSiBridge is used for the finite-element analysis and Matlab verifies the limit states based on the load effects from CSiBridge and the bridge resistance evaluation. After this process, a new actualized Pareto front is presented. These solutions must be feasible. Therefore, HS solutions belonging to the Pareto set in the previous steps can have another ranking after this step. And on the contrary, HS solutions with ranking greater than one can constitute the Pareto set.

2.2.4 Step 4. Exact Pareto front

The last step carries out a multi-objective optimization through an exact method. This process starts with the actualized HM. A new harmony memory with HMS solutions is generated based on the HS strategy. Each new harmony or solution generated is analyzed and verified. Only feasible solutions are saved. The harmony memory is updated with the solutions of highest ranking. Note that when the number of solutions with ranking equal to one that is, belonging to the Pareto front, is greater than the value of HMS, the HMS value is increased to the number of Pareto solutions. The optimization process finishes after ten consecutive harmony memory updates with a difference in hypervolume value of less than 0.0005.

3. Results

3.1. Results of ANN

The results of the ANNs are summarized in Table 5. The coefficient of determination R^2 and the MSE analyze, the relation between the output and targets and the network's performance. Values of R^2 vary between 0.912 and 0.999 and MSE takes values between 0.0001 and 0.088.

3.2. Results of approximate Pareto set

ANN was combined with the multi-objective HS to obtain an approximate Pareto set. Ten different cases were studied regarding the algorithm parameters and the coefficient of penalty function (see Table 4). The hypervolume was used as a metric to compare the results. This metric evaluates a combination of convergence and spread of solutions. The results in Table 6 show that Case 10 presents the greatest hypervolume. This case corresponds to the progressive diversification-intensification strategy. Note that Cases 1–3 present increasing values of HMCR, as do Cases 4–6. In all of them, the case with the greatest hypervolume is the last one. Therefore, it is worth noting that the greatest HMCR value performs better for this structural problem. When HMCR is equal to one, the random selection of the value of the variables becomes unlikely. Regarding fixing the memory consideration to one solution, Cases 4–6 have better results than Cases 1–3. This means that combining variables from different solutions is less effective than taking only one solution and perturbing some members. However, Case 10, which allows the combination of solutions and random selection in the beginning, has the best results. Concerning the penalty function, Cases 7-9 analyze a higher value of K_p coefficient. The hypervolume is smaller when increasing the cost of unfeasible solutions with K_p equal to 1.1. As this parameter worsens the solutions, the hypervolume is expected to have a smaller value. Thus, Case 8 was also studied in the next step to determine whether this case is definitely worse than Case 10.

3.3. Results of the updated Pareto set

When the approximate Pareto set is actualized, the limit state coefficients are modified. In turn, the objective values and the hypervolume change. This step is carried out in Cases 8 and 10. The hypervolume of Case 8 was reduced from 0.6589 to 0.6499 and the hypervolume of Case 10 varied from 0.6748 to 0.6520. Unsurprisingly, the hypervolume difference of Case 8 is smaller, since this case imposes a higher penalty on unfeasible solutions. Even so, after the updating, the hypervolume remains smaller in Case 10. Therefore, Case 10 is used to carry out the following step.

3.4. Results of exact Pareto front

The last step improved the Pareto performance from a hypervolume of 0.652 to 0.668 (see Fig. 5). The results show a percentage of exact function evaluations of about 37% when the exact evaluations for ANN training are taken into account. However, if the ANN training data are not considered, the percentage of exact function evaluations is 27%. It is worth noting the importance of this result, since the average time for obtaining an exact feasible solution is about 1500 s, while obtaining a solution through ANN takes about 4 s. In addition, it should be noted that the ANN training for the 17 neural networks consumes about 7 min. The total computation time depends on the computer, the software and the technique used, among others. In our case, the personal computer has an INTEL® CoreTM i7-3820 CPU processor and 3.6 GHz. It should be noted that 82% of the computation time for obtaining an exact feasible solution is spent in the finite element analysis and exporting of results.

The Pareto set (see Fig. 6) contains the solutions that cannot be improved without worsening the value of one objective. This set provides trade-off solutions from which the designer can select the most desirable one. Some solutions require higher cost of production of materials and construction of the bridge, but these solutions have a longer lifetime thanks to the higher corrosion initiation time and improved safety. Consequently, they will incur lower maintenance and repair costs. Codes recommend the same service life target and safety level for all road bridges. However, this paper gives multiple alternatives that can easily be adjusted to each need.

The relationship between the cost and the overall safety factor presents a parabolic fit. This relation is maintained for each corrosion initiation time. Note that the corrosion initiation time is limited to 500 years. Each of these solutions is the cheapest for the safety and durability level. Likewise, when choosing a safety and durability target, it is possible to know the best cross-section geometry, concrete grade, reinforcement, and post-tensioning steel. Note that there are solutions whose cost is smaller than €500000 that have an overall safety factor of around 1.5 and a maximum corrosion initiation time. This means that with a small cost increment, the safety and durability can be greatly improved.

Fig. 7 shows the Pareto front, highlighting the concrete grade of these solutions. Just solutions that use 35, 45, 55, 70 and 90 MPa concrete are highlighted. The variables with influence over the corrosion initiation time are the concrete strength and the concrete cover. On analyzing the results according to the concrete strength, Fig. 7 illustrates a tendency towards increasing corrosion time with increasing concrete strength. The average corrosion initiation times are 36.3, 88.3, 343.7 and 500 years for 35, 45, 55, 70, and 90 MPa, respectively. However, the concrete strength and overall safety factor do not present a clear relationship. The same safety range can be obtained with different concrete grades.

Regarding the concrete cover effect (see Fig. 8), solutions with concrete cover of 30, 35, 60 and 75 mm are analyzed. It is worth noting that an increment in concrete cover has an effect on the corrosion initiation time that depends on the value of concrete strength. This relationship is represented in Fig. 9. Considering a linear relation between corrosion initiation time and concrete cover, both the slope and y-intercept increase with the concrete strength. Therefore, for low grades of concrete, an increment in concrete cover has less effect on the corrosion initiation time, compared to high-strength concrete. Likewise, Fig. 9 shows big differences between the corrosion initiation time of low and high-strength concrete. As concrete strength generally has more economic impact than concrete cover, increments in concrete strength favors strategies of higher service life targets and increments in concrete cover favors strategies of lower service life targets. Thus, there are optimum bridge solutions with the maximum corrosion initiation time that use high-strength concrete with the minimum cover. However, the opposite case is not obtained. In conclusion, an optimum selection of a concrete cover and concrete strength can achieve the durability and cost goals.

4. Concluding remarks

In this paper, post-tensioned concrete box-girder road bridges are optimized, considering the cost, the overall safety factor, and the corrosion initiation time as objectives. The durability is transformed from a constraint to an objective with the aim of designing for longevity and reduced long-term impacts. In this regard, this study gives the opportunity to explore new designs without limiting the design by predefined constraints on durability measures. The multi-objective optimization aims to find designs with lower cost, longer corrosion initiation time and improved safety. Pareto front provides trade-off solutions with a little cost increment but these solutions have a longer lifetime and improved safety, compared to the minimum cost solution. However, as the number of objectives increases, the problem becomes more complex and the computing time increases. In addition, the bridge analysis is carried out through a finite-element program with a substantially increased time. This paper proposes a methodology to reduce the number of exact evaluations by using ANN.

The methodology implements four stages. Firstly, the ANN is trained by the limit state data of previous evaluations of the same bridge problem, even though the objective functions are different. The aim is to learn about the relationship between the variables and the limit state coefficient, since this part is the most computationally intensive. Secondly, a multi-objective HS is combined with ANN to obtain an approximate Pareto front that provides a good search direction. In this step, several cases are considered to study the algorithm parameters and the penalty function. Then, the third step actualizes the Pareto set of solutions with a finite-element analysis, limit state verification, and objective evaluation. The unfeasible solutions do not proceed to the next step. Finally, the multi-objective optimization problem is solved with exact evaluations.

The results of ANN give values of the coefficient of determination R^2 between 0.912 and 0.999. The study of the algorithm parameters shows the best results for the combination of parameters that follow a transition from diversification to intensification. The progressive elimination of the combination of solutions and the random selection achieve the highest hypervolume measure. Finally, the methodology show a percentage of exact function evaluations of about 37% or 27%, depending on whether or not the training data are taken into account. This takes on far greater significance when the computational time is reduced from about 1500 s when obtaining an exact feasible solution to 4 s when using ANN. The findings indicate that ANN is a good tool to reproduce the structure response and reduce the time cost. However, the last steps need finer models to converge closer to the true Pareto front.

Pareto front provides a trade-off between the cost, the overall safety factor, and the corrosion initiation time. The designer can select the cheapest solution for the safety and durability target. Both the effect of increasing the concrete strength and concrete cover is not the same for each concrete grade. For low grades of concrete, an increment in both variables has less effect on the corrosion initiation time, compared to high strength concrete. While increments in concrete strength favors strategies of higher service life targets, increments in concrete cover favors strategies of lower service life targets. A good combination of both concrete strength and concrete cover could achieve the durability and cost goals.

Acknowledgments

The authors acknowledge the financial support of the Spanish Ministry of Economy and Competitiveness, along with FEDER funding (BRIDLIFE Project: BIA2014-56574-R) and the

Research and Development Support Program of Universitat Politècnica de València (PAID-02-15).

References

Alberdi R, Khandelwal K (2015) Comparison of robustness of metaheuristic algorithms for steel frame optimization. Eng Struct 102:40–60. doi: 10.1016/j.engstruct.2015.08.012

Beume N, Naujoks B, Emmerich M (2007) SMS-EMOA: Multiobjective selection based on dominated hypervolume. Eur J Oper Res 181:1653–1669. doi: 10.1016/j.ejor.2006.08.008

Cai H, Aref AJ (2015) A genetic algorithm-based multi-objective optimization for hybrid fiber reinforced polymeric deck and cable system of cable-stayed bridges. Struct Multidiscip Optim 52:583–594. doi: 10.1007/s00158-015-1266-4

Cao MS, Pan LX, Gao YF, Novák D, Ding ZC, Lehký D, Li XL (2015) Neural network ensemble-based parameter sensitivity analysis in civil engineering systems. Neural Comput Appl 1–8. doi: 10.1007/s00521-015-2132-4

Chatterjee S, Sarkar S, Hore S, Dey N, Ashour AS, Balas VE (2016) Particle swarm optimization trained neural network for structural failure prediction of multistoried RC buildings. Neural Comput. Appl. 1–12. doi: 10.1007/s00521-016-2190-2

Coello CAC (2002) Theoretical and numerical constraint-handling techniques used with evolutionary algorithms: a survey of the state of the art. Comput Methods Appl Mech Eng 191:1245–1287. doi: 10.1016/S0045-7825(01)00323-1

Coello CAC, Lamont GB, Veldhuizen DA Van (2006) Evolutionary algorithms for solving multi-objective problems. Springer-Verlag New York, Inc.

Computers and Structures Inc CSiBridge. Integrated 3D bridge analysis, design and rating.

Deb K (2011) Multi-objective optimisation using evolutionary algorithms: An introduction. In: Wang L, Ng AHC, Deb K (eds) Multi-objective Evolutionary Optimisation for Product Design and Manufacturing. Springer London, London, pp 3–34

Deb K, Nain PKS (2007) An evolutionary multi-objective adaptive meta-modeling procedure using artificial neural networks. In: Yang S, Ong Y-S, Jin Y (eds) Evolutionary Computation in Dynamic and Uncertain Environments. Springer Berlin Heidelberg, Berlin, Heidelberg, pp 297–322

Dong Y, Frangopol DM, Saydam D (2013) Time-variant sustainability assessment of seismically vulnerable bridges subjected to multiple hazards. Earthq Eng Struct Dyn 42:1451–1467. doi: 10.1002/eqe.2281

Emmerich M, Naujoks B (2004) Metamodel assisted multiobjective optimisation strategies and their application in airfoil design. In: Parmee IC (ed) Adaptive Computing in Design and Manufacture VI. Springer London, London, pp 249–260

European Committee for Standardisation (2003) EN 1991-2:2003. Eurocode 1: Actions on structures-Part 2: Traffic loads bridges.

European Committee for Standardisation (2005) EN1992-2:2005. Eurocode 2: Design of concrete structures- Part 2: Concrete Bridge-Design and detailing rules. Brussels

Fomento M (2011) IAP-11: Code on the actions for the design of road bridges. Ministerio de Fomento, Madrid, Spain

Fomento M (2008) EHE-08: Code on structural concrete. Ministerio de Fomento, Madrid, Spain

García-Segura T, Yepes V (2016) Multiobjective optimization of post-tensioned concrete box-girder road bridges considering cost, CO2 emissions, and safety. Eng Struct 125:325–336.

doi: 10.1016/j.engstruct.2016.07.012

García-Segura T, Yepes V, Alcalá J (2014a) Life cycle greenhouse gas emissions of blended cement concrete including carbonation and durability. Int J Life Cycle Assess 19:3–12. doi: 10.1007/s11367-013-0614-0

García-Segura T, Yepes V, Alcalá J, Pérez-López E (2015) Hybrid harmony search for sustainable design of post-tensioned concrete box-girder pedestrian bridges. Eng Struct 92:112–122. doi: 10.1016/j.engstruct.2015.03.015

García-Segura T, Yepes V, Martí JV, Alcalá J (2014b) Optimization of concrete I-beams using a new hybrid glowworm swarm algorithm. Lat Am J Solids Struct 11:1190–1205. doi: 10.1590/S1679-78252014000700007

Geem ZW, Kim JH, Loganathan G V. (2001) A new heuristic optimization algorithm: Harmony search. Simulation 76:60–68.

Giannakoglou KC (2002) Design of optimal aerodynamic shapes using stochastic optimization methods and computational intelligence. Prog Aerosp Sci 38:43–76. doi: 10.1016/S0376-0421(01)00019-7

Hare W, Nutini J, Tesfamariam S (2013) A survey of non-gradient optimization methods in structural engineering. Adv Eng Softw 59:19–28. doi: 10.1016/j.advengsoft.2013.03.001

Marti-Vargas JR, Ferri FJ, Yepes V (2013) Prediction of the transfer length of prestressing strands with neural networks. Comput Concr 12:187–209. doi: 10.12989/cac.2013.12.2.187

Martí JV, García-Segura T, Yepes V (2016) Structural design of precast-prestressed concrete U-beam road bridges based on embodied energy. J Clean Prod 120:231–240. doi: 10.1016/j.jclepro.2016.02.024

Martí J V., Yepes V, González-Vidosa F (2015) Memetic algorithm approach to designing precast-prestressed concrete road bridges with steel fiber reinforcement. J Struct Eng 141:4014114. doi: 10.1061/(ASCE)ST.1943-541X.0001058

Martinez-Martin FJ, Gonzalez-Vidosa F, Hospitaler A, Yepes V (2012) Multi-objective optimization design of bridge piers with hybrid heuristic algorithms. J Zhejiang Univ Sci A 13:420–432. doi: 10.1631/jzus.A1100304

Martini K (2011) Harmony search method for multimodal size, shape, and topology optimization of structural frameworks. J Struct Eng 137:1332–1339. doi: 10.1061/(ASCE)ST.1943-541X.0000378

McGee R (1999) Modeling of durability performance of Tasmanian bridges. In: Melchers R, M.G S (eds) Applications of statistics and probability: civil engineering, reliability and risk analysis. A.A. Balkema, Rotterdam, pp 297–306

Papadakis VG, Roumeliotis AP, Fardis MN, Vagenas CG (1996) Mathematical modelling of chloride effect on concrete du-rability and protection measures. In: Dhir RK, Jones MR (eds) Concrete repair, rehabilitation and protection. E&FN Spon, London, pp 165–174

Paya I, Yepes V, González-Vidosa F, Hospitaler A (2008) Multiobjective optimization of reinforced concrete building frames by simulated annealing. Comput Civ Infrastruct Eng 23:596–610. doi: 10.1111/j.1467-8667.2008.00561.x

Protopapadakis E, Schauer M, Pierri E, et al (2016) A genetically optimized neural classifier applied to numerical pile integrity tests considering concrete piles. Comput Struct 162:68–79. doi: 10.1016/j.compstruc.2015.08.005

Quaglia CP, Yu N, Thrall AP, Paolucci S (2014) Balancing energy efficiency and structural performance through multi-objective shape optimization: Case study of a rapidly deployable origami-inspired shelter. Energy Build 82:733–745. doi: 10.1016/j.enbuild.2014.07.063

Ricart J, Hüttemann G, Lima J, Barán B (2011) Multiobjective harmony search algorithm proposals. Electron Notes Theor Comput Sci 281:51–67. doi: 10.1016/j.entcs.2011.11.025

Sanad A, Saka MP (2001) Prediction of ultimate shear strength of reinforced-concrete deep beams using neural networks. J Struct Eng 127:818–828. doi: 10.1061/(ASCE)0733-9445(2001)127:7(818)

Sarma KC, Adeli H (1998) Cost optimization of concrete structures. J Struct Eng 124:570–578. doi: 10.1061/(ASCE)0733-9445(1998)124:5(570)

Shi X (2016) Experimental and modeling studies on installation of arc sprayed Zn anodes for protection of reinforced concrete structures. Front Struct Civ Eng 10:1–11. doi: 10.1007/s11709-016-0312-7

Sreehari VM, Maiti DK (2016) Buckling load enhancement of damaged composite plates under hygrothermal environment using unified particle swarm optimization. Struct Multidiscip Optim 1–11. doi: 10.1007/s00158-016-1498-y

Torres-Machi C, Chamorro A, Pellicer E, et al (2015) Sustainable pavement management: Integrating economic, technical, and environmental aspects in decision making. Transp Res Rec J Transp Res Board 2523:56–63. doi: 10.3141/2523-07

Vu KAT, Stewart MG (2000) Structural reliability of concrete bridges including improved chloride-induced corrosion models. Struct Saf 22:313–333. doi: 10.1016/S0167-4730(00)00018-7

Xu H, Gao XZ, Wang T, Xue K (2010) Harmony search optimization algorithm: application to a reconfigurable mobile robot prototype. In: Geem ZW (ed) Recent advances in harmony search algorithm. Springer Berlin Heidelberg, Berlin, Heidelberg, pp 11–22

Yepes V, García-Segura T, Moreno-Jiménez JM (2015a) A cognitive approach for the multi-objective optimization of RC structural problems. Arch Civ Mech Eng 15:1024–1036. doi: 10.1016/j.acme.2015.05.001

Yepes V, Martí JV, García-Segura T (2015b) Cost and CO2 emission optimization of precast–prestressed concrete U-beam road bridges by a hybrid glowworm swarm algorithm. Autom Constr 49:123–134. doi: 10.1016/j.autcon.2014.10.013

Zavala GR, Nebro AJ, Luna F, Coello Coello CA (2013) A survey of multi-objective metaheuristics applied to structural optimization. Struct Multidiscip Optim 49:537–558. doi: 10.1007/s00158-013-0996-4

Zavrtanik N, Prosen J, Tušar M, Turk G (2016) The use of artificial neural networks for modeling air void content in aggregate mixture. Autom Constr 63:155–161. doi: 10.1016/j.autcon.2015.12.009

Zitzler E, Thiele L (1998) Multiobjective optimization using evolutionary algorithms - a comparative case study. In: Eiben AE, Bäck T, Schoenauer M, Schwefel H-P (eds) Conference on parallel problem solving from nature- PPSN V. Springer Berlin Heidelberg, Amsterdam, The Netherlands, pp 292–301

Table 1. Unit prices

Unit measurements	Cost (€)
Square meter of formwork	33.81
Kilogram of steel (B-500-S)	1.16
Kilogram of prestressing steel (Y1860-S7)	3.40
Cubic meter of concrete 35 MPa	104.57
Cubic meter of concrete 40 MPa	109.33
Cubic meter of concrete 45 MPa	114.10
Cubic meter of concrete 50 MPa	118.87
Cubic meter of concrete 55 MPa	123.64
Cubic meter of concrete 60 MPa	128.41
Cubic meter of concrete 70 MPa	137.95
Cubic meter of concrete 80 MPa	147.49
Cubic meter of concrete 90 MPa	157.02
Cubic meter of concrete 100 MPa	166.56

Table 2. Parameters of the random variables associated with corrosion

Random Variables	**Model type**
Model error (*D*)	Normal (μ = 1, COV = 0.2)
C_o	Lognormal (μ = 2.95, COV = 0.3)
C_r	Uniform (0.6–1.2)
Cover	Normal (μ = c_c, COV = 0.25)

Table 3. Aggregate-to-cement ratio and water-cement ratio for each concrete grade

Concrete grade	a/c	w/c
Concrete 35 MPa	6.45	0.54
Concrete 40 MPa	6.03	0.5
Concrete 45 MPa	5.47	0.45
Concrete 50 MPa	4.66	0.4
Concrete 55 MPa	3.92	0.35
Concrete 60 MPa	3.64	0.33
Concrete 70 MPa	3.56	0.31
Concrete 80 MPa	3.55	0.3
Concrete 90 MPa	3.52	0.3
Concrete 100 MPa	3.22	0.3

Table 4. Algorithm parameters for each case of Step 2.

		HMS	PAR	HMCR	Fix memory consideration	K_p
Case 1		200	0.4	0.7	No	1
Case 2		200	0.4	0.85	No	1
Case 3		200	0.4	1	No	1
Case 4		200	0.4	0.7	Yes	1
Case 5		200	0.4	0.85	Yes	1
Case 6		200	0.4	1	Yes	1
Case 7		200	0.4	0.7	Yes	1.1
Case 8		200	0.4	0.85	Yes	1.1
Case 9		200	0.4	1	Yes	1.1
Case 10	Phase 1: 2500 iterations	200	0.4	0.7	No	1
	Phase 2: 2500 iterations	200	0.4	0.7	Yes	1
	Phase 3: 15000 iterations	200	0.4	1	Yes	1

Table 5. ANN results

Limit state	**MSE**	**R^2**
Stresses during prestressing	0.0213	0.976
Serviceability stresses	0.0039	0.996
Deflection (Fomento 2008)	0.0036	0.996
Deflection (Fomento 2011)	0.0001	0.999
Flexure	0.0574	0.942
Minimum flexure reinforcement	0.0704	0.930
Shear	0.0063	0.993
Minimum shear reinforcement	0.0116	0.988
Shear between web and flanges	0.0384	0.960
Torsion: longitudinal reinforcement	0.0096	0.990
Torsion: transverse reinforcement	0.0270	0.973
Minimum torsion reinforcement	0.0407	0.959
Torsion combined with shear	0.0012	0.999
Torsion combined with tension	0.0408	0.958
Transverse flexion	0.0479	0.952
Minimum transverse reinforcement	0.0877	0.912
Transverse shear	0.0627	0.937

Table 6. Results of approximate Pareto set for each case

	Case 1	**Case 2**	**Case 3**	**Case 4**	**Case 5**	**Case 6**	**Case 7**	**Case 8**	**Case 9**	**Case 10**
Hypervolume	0.6286	0.6322	0.6373	0.6504	0.6612	0.6744	0.6225	0.6589	0.6583	0.6748

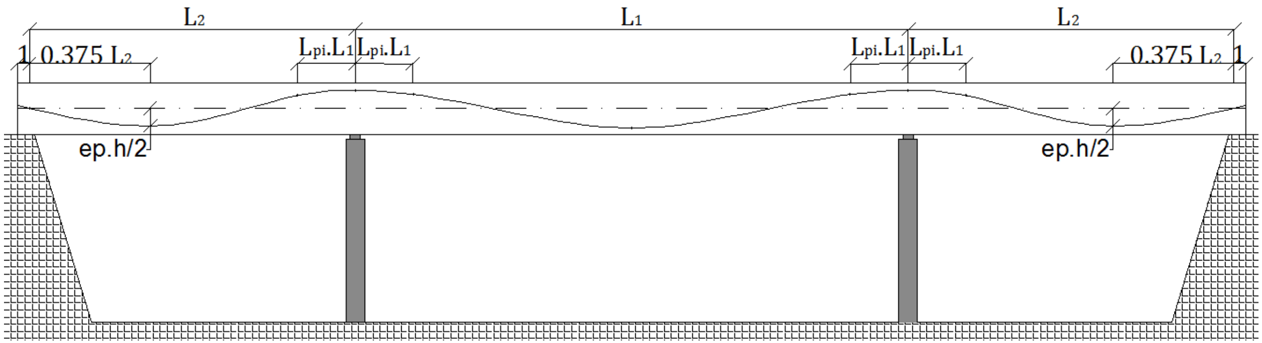

Fig. 1. Bridge elevation and post-tensioned steel

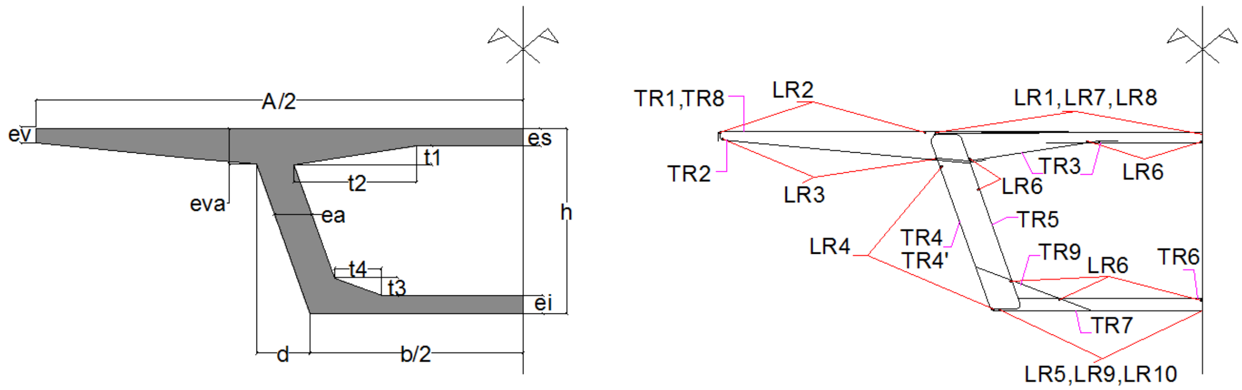

589

590 **Fig. 2.** Geometric and reinforcing steel variables

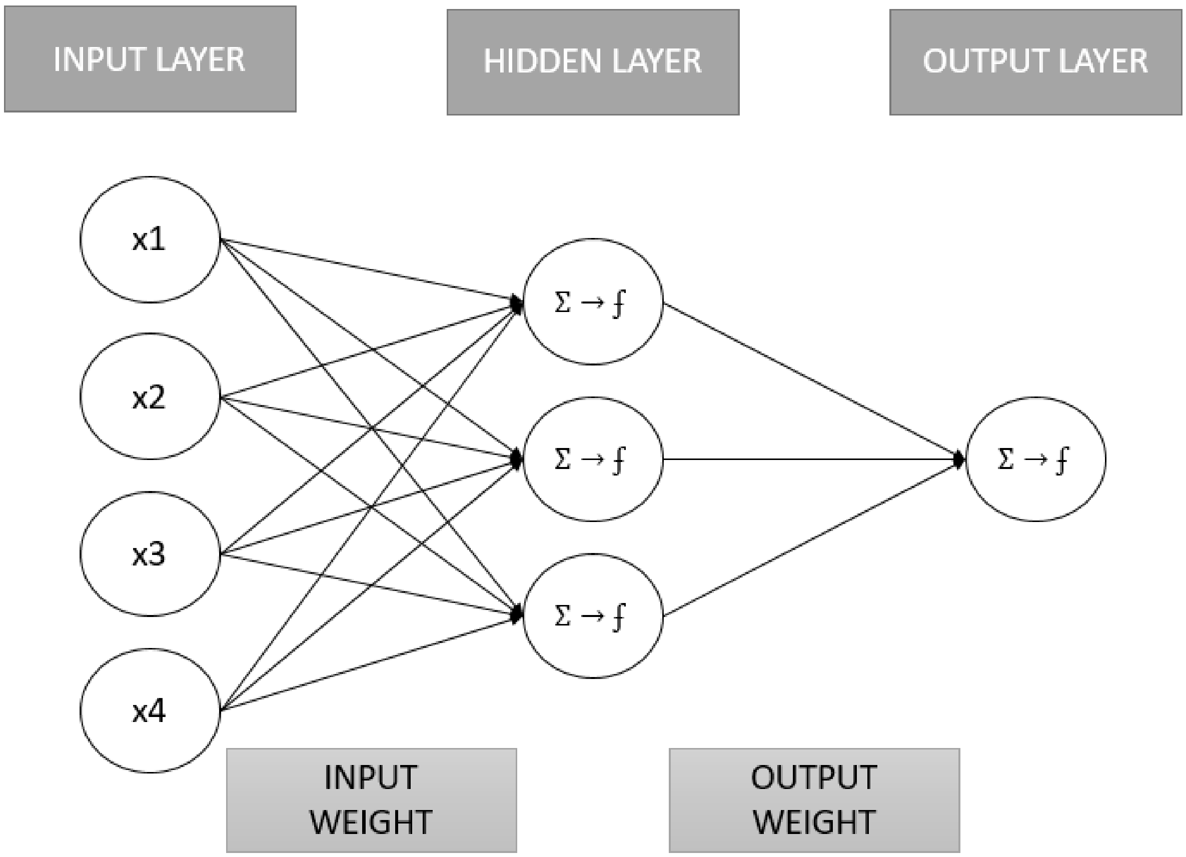

Fig. 3. Multilayer feedforward network

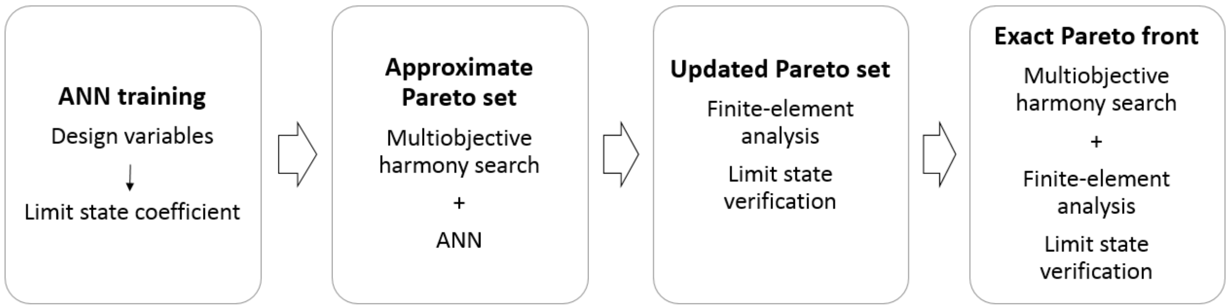

Fig. 4. Basic steps of the integrated multi-objective harmony search with artificial neural networks

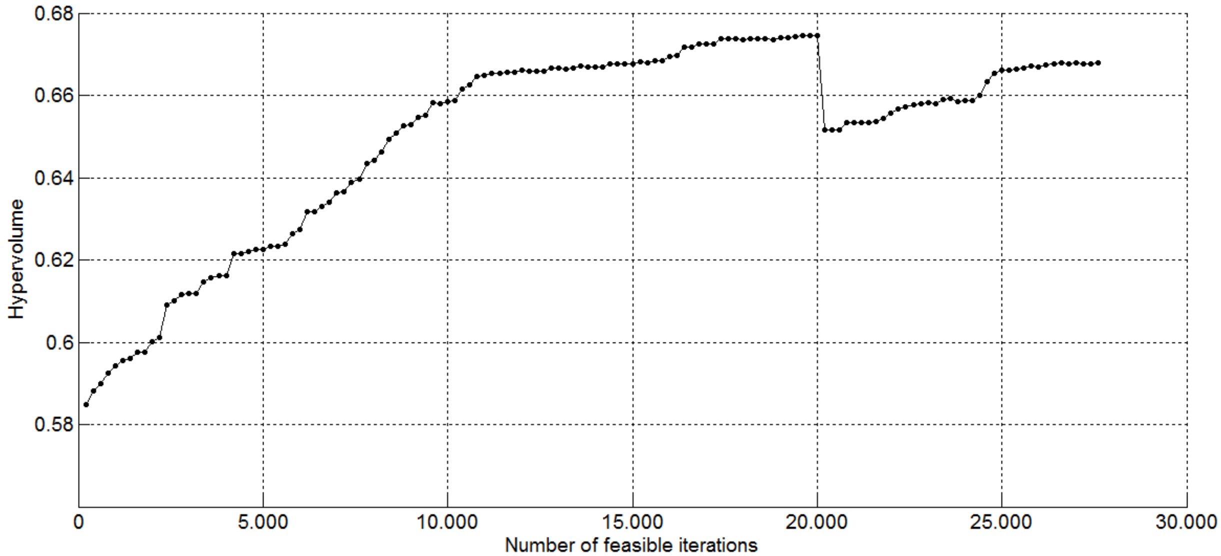

Fig. 5. Evolution of Pareto front through hypervolume evaluation

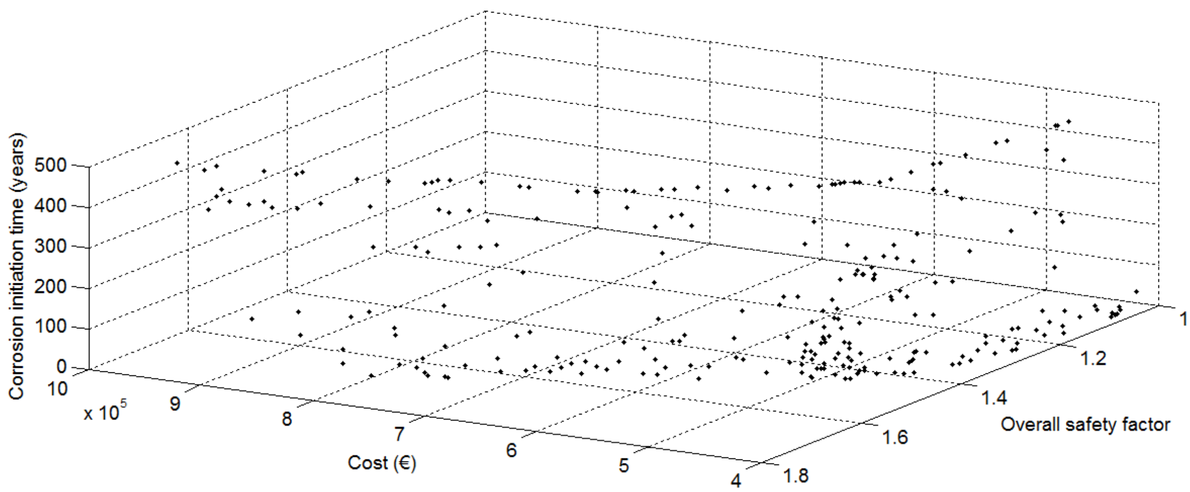

Fig. 6. Pareto optimal solutions for cost, overall safety factor and corrosion initiation time

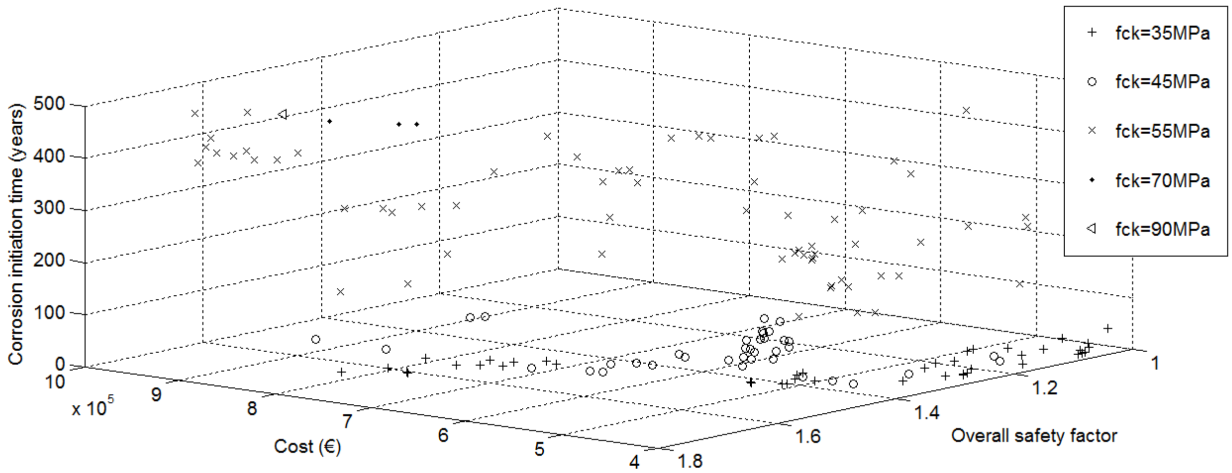

Fig. 7. Pareto optimal solutions according to the concrete grade

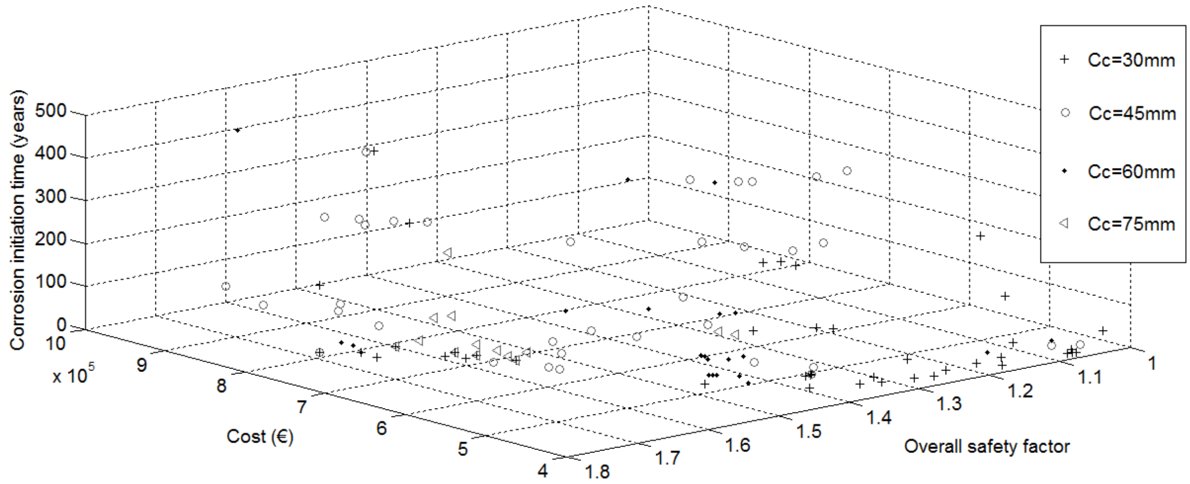

Fig. 8. Pareto optimal solutions according to the concrete cover

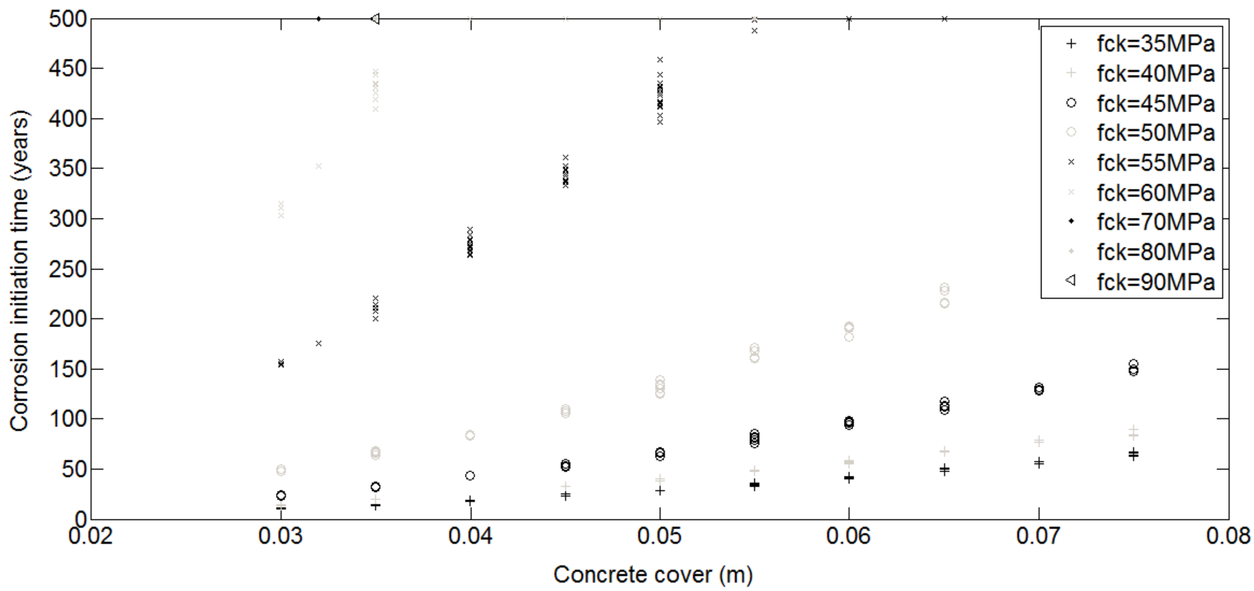

603

604 **Fig. 9.** Corrosion initiation time according to concrete cover and concrete strength